



**Defense Threat Reduction Agency  
8725 John J. Kingman Road, MS  
6201 Fort Belvoir, VA 22060-6201**



**DTRA-TR-13-045**

# TECHNICAL REPORT

## **Monte Carlo Modeling of the Initial Radiation Emitted by a Nuclear Device in the National Capital Region**

DISTRIBUTION A. Approved for public release: distribution is unlimited.

July 2013

Prepared by:

Human Survivability Research and  
Development Integrated Program Team



THIS PAGE IS INTENTIONALLY LEFT BLANK.

REPORT DOCUMENTATION PAGE				Form Approved OMB No. 0704-0188	
<p>Public reporting burden for this collection of information is estimated to average 1 hour per response, including the time for reviewing instructions, searching data sources, gathering and maintaining the data needed, and completing and reviewing the collection of information. Send comments regarding this burden estimate or any other aspect of this collection of information, including suggestions for reducing this burden to Washington Headquarters Service, Directorate for Information Operations and Reports, 1215 Jefferson Davis Highway, Suite 1204, Arlington, VA 22202-4302, and to the Office of Management and Budget, Paperwork Reduction Project (0704-0188) Washington, DC 20503.</p> <p><b>PLEASE DO NOT RETURN YOUR FORM TO THE ABOVE ADDRESS.</b></p>					
1. REPORT DATE (DD-MM-YYYY) 01-07-2013		2. REPORT TYPE Technical Report		3. DATES COVERED (From – To)	
4. TITLE AND SUBTITLE Monte Carlo Modeling of the Initial Radiation Emitted by an Improvised Nuclear Device in the National Capital Region				5a. CONTRACT NUMBER DTRA01-03-D-0014-0038	
				5b. GRANT NUMBER	
				5c. PROGRAM ELEMENT NUMBER	
6. AUTHOR(S) Kevin Kramer, Andy Li, Joe Madrigal, Brian Sanchez, and Kyle Millage				5d. PROJECT NUMBER	
				5e. TASK NUMBER	
				5f. WORK UNIT NUMBER	
7. PERFORMING ORGANIZATION NAME(S) AND ADDRESS(ES) Applied Research Associates, Inc. 801 N. Quincy St., Suite 700 Arlington, VA 22203				8. PERFORMING ORGANIZATION REPORT NUMBER DTRA-TR-13-045	
9. SPONSORING / MONITORING AGENCY NAME(S) AND ADDRESS(ES) Defense Threat Reduction Agency 8725 John J. Kingman Road, MS 6201 Fort Belvoir, VA 22060-6201				10. SPONSOR/MONITOR'S ACRONYM(S) DTRA J9NTSN	
				11. SPONSOR/MONITOR'S REPORT NUMBER(S)	
12. DISTRIBUTION / AVAILABILITY STATEMENT DISTRIBUTION A: Approved for public release; distribution is unlimited.					
13. SUPPLEMENTARY NOTES					
14. ABSTRACT This document presents the results from an analysis of the impact of urban terrain on the transport of initial radiation from a low yield nuclear device in the National Capital Region. The objective of the work was to use high-fidelity models of radiation propagation to quantify the attenuation and scattering caused by an urban landscape. The results are based on simulated data from the propagation of initial photons and neutrons emitted from a 10 kiloton fission device, detonated at ground level, through both an open-field and urban environment. Scattered radiation from atmosphere, ground, and urban structures is also simulated in the models. Data was derived from calculations using the three-dimensional Monte Carlo radiation transport code MCNP (Monte Carlo N-Particle). The emphasis of this report is on the radiation dose that would be received by individuals, and how that dose is perturbed by an urban environment. Consequently, radiation dose to tissue is reported and neutron doses are not modified to account for their relative biological effectiveness. The results shown in this report indicate the urban terrain provides significant attenuation of the initial neutron and photon emissions. These results show that the dose is reduced to between 20-30% of the open field dose depending on the building characteristics.					
15. SUBJECT TERMS Radiation Transport      Nuclear Detonation      Initial Radiation      Urban Terrain      Dose Estimate					
16. SECURITY CLASSIFICATION OF:			17. LIMITATION OF ABSTRACT  Unlimited	18. NUMBER OF PAGES  41	19a. NAME OF RESPONSIBLE PERSON Paul K. Blake, PhD
a. REPORT U	b. ABSTRACT U	a. THIS PAGE U			19b. TELEPHONE NUMBER (include area code) 703 767-3433

Standard Form 298 (Rev. 8-98) Prescribed by  
ANSI Std. Z39.18

## UNIT CONVERSION TABLE

U.S. customary units to and from international units of measurement\*

U.S. Customary Units	Multiply by 		International Units
	 Divide by <sup>†</sup>		
<b>Length/Area/Volume</b>			
inch (in)	2.54	$\times 10^{-2}$	meter (m)
foot (ft)	3.048	$\times 10^{-1}$	meter (m)
yard (yd)	9.144	$\times 10^{-1}$	meter (m)
mile (mi, international)	1.609 344	$\times 10^3$	meter (m)
mile (nmi, nautical, U.S.)	1.852	$\times 10^3$	meter (m)
barn (b)	1	$\times 10^{-28}$	square meter (m <sup>2</sup> )
gallon (gal, U.S. liquid)	3.785 412	$\times 10^{-3}$	cubic meter (m <sup>3</sup> )
cubic foot (ft <sup>3</sup> )	2.831 685	$\times 10^{-2}$	cubic meter (m <sup>3</sup> )
<b>Mass/Density</b>			
pound (lb)	4.535 924	$\times 10^{-1}$	kilogram (kg)
atomic mass unit (AMU)	1.660 539	$\times 10^{-27}$	kilogram (kg)
pound-mass per cubic foot (lb ft <sup>-3</sup> )	1.601 846	$\times 10^1$	kilogram per cubic meter (kg m <sup>-3</sup> )
pound-force (lbf avoirdupois)	4.448 222		newton (N)
<b>Energy/Work/Power</b>			
electronvolt (eV)	1.602 177	$\times 10^{-19}$	joule (J)
erg	1	$\times 10^{-7}$	joule (J)
kiloton (kT) (TNT equivalent)	4.184	$\times 10^{12}$	joule (J)
British thermal unit (Btu) (thermochemical)	1.054 350	$\times 10^3$	joule (J)
foot-pound-force (ft lbf)	1.355 818		joule (J)
calorie (cal) (thermochemical)	4.184		joule (J)
<b>Pressure</b>			
atmosphere (atm)	1.013 250	$\times 10^5$	pascal (Pa)
pound force per square inch (psi)	6.984 757	$\times 10^3$	pascal (Pa)
<b>Temperature</b>			
degree Fahrenheit (°F)	[T(°F) − 32]/1.8		degree Celsius (°C)
degree Fahrenheit (°F)	[T(°F) + 459.67]/1.8		kelvin (K)
<b>Radiation</b>			
curie (Ci) (activity of radionuclides)	3.7	$\times 10^{10}$	s <sup>−1‡</sup>
air exposure (roentgen)	2.579 760	$\times 10^{-4}$	coulomb per kilogram (C kg <sup>−1</sup> )
absorbed dose (rad)	1	$\times 10^{-2}$	J kg <sup>−1§</sup>
equivalent and effective dose (rem)	1	$\times 10^{-2}$	J kg <sup>−1**</sup>

\* Specific details regarding the implementation of SI units may be viewed at <http://www.bipm.org/en/si/>.

† Multiply the U.S. customary unit by the factor to get the international unit. Divide the international unit by the factor to get the U.S. customary unit.

‡ The special name for the SI unit of the activity of a radionuclide is the becquerel (Bq). (1 Bq = 1 s<sup>-1</sup>).

§ The special name for the SI unit of absorbed dose is the gray (Gy). (1 Gy = 1 J kg<sup>-1</sup>).

\*\* The special name for the SI unit of equivalent and effective dose is the sievert (Sv). (1 Sv = 1 J kg<sup>-1</sup>).

## TABLE OF CONTENTS

<b>LIST OF FIGURES .....</b>	<b>vii</b>
<b>LIST OF TABLES .....</b>	<b>ix</b>
<b>1.0 INTRODUCTION .....</b>	<b>1</b>
<b>2.0 MODEL DESCRIPTION.....</b>	<b>3</b>
<b>3.0 NUMERICAL METHODS.....</b>	<b>7</b>
<b>4.0 SOURCE DESCRIPTION.....</b>	<b>9</b>
<b>5.0 RESULTS .....</b>	<b>11</b>
5.1 RECTANGULAR MESH TALLY RESULTS .....	11
5.2 DATA ANALYSIS.....	14
<b>6.0 DISCUSSION .....</b>	<b>23</b>
6.1 ANALYSIS OF DOSE REDUCTION .....	23
6.2 RECOGNIZED HSRD MODEL LIMITATIONS .....	23
6.3 ABSORBED DOSE VERSUS EQUIVALENT DOSE .....	23
<b>7.0 CONCLUSIONS .....</b>	<b>25</b>
<b>8.0 ACKNOWLEDGEMENTS .....</b>	<b>27</b>
<b>9.0 REFERENCES.....</b>	<b>29</b>
<b>APPENDICES.....</b>	<b>31</b>
<b>A. ATMOSPHERIC COMPOSITION AND DENSITY .....</b>	<b>32</b>
<b>B. MCNP PHYSICS OPTIONS .....</b>	<b>33</b>
<b>C. HAZUS BUILDING TYPES.....</b>	<b>34</b>
<b>D. ABBREVIATIONS, ACRONYMS AND SYMBOLS .....</b>	<b>36</b>

THIS PAGE IS INTENTIONALY LEFT BLANK.

## LIST OF FIGURES

Figure 2-1. Washington, D.C. represented on a 3-D lattice model. The different colors correspond to different Hazus building types. ....	4
Figure 2-2. Example set of buildings and their city block labels from the FEMA Hazus database. ....	4
Figure 2-3. Different combinations of building and air lattice elements which each contain different exterior wall arrangements .....	5
Figure 2-4. An example section of a building model representing four different 5 m x 5 m x 5 m lattice elements.....	6
Figure 3-1. Values of weight window lower bounds for DC urban simulation with the photon source .....	8
Figure 4-1. Neutron energy spectrum used in simulation. Derived from isotropic version of Little Boy bomb used on Hiroshima (White, 2001) .....	9
Figure 4-2. Photon energy spectrum used in simulation. Derived from isotropic version of Little Boy bomb used on Hiroshima (White, 2001) .....	10
Figure 5-1. Open field total absorbed dose.....	12
Figure 5-2. Urban horizontal total absorbed dose.....	12
Figure 5-3. Urban horizontal neutron absorbed dose.....	13
Figure 5-4. Urban horizontal photon absorbed dose from both leakage photons and secondary photons from neutron interactions .....	13
Figure 5-5. The ratio of urban horizontal absorbed dose to open field horizontal absorbed dose.....	14
Figure 5-6. The model's city geometry showing the buildings used to calculate the outside-of-building dose.....	15
Figure 5-7. Open and outside-of-buildings urban scenario dose fall-offs. ....	16
Figure 5-8. Total Urban-to-Open field dose ratio at locations outside buildings for the four quadrants from Figure 5-5 .....	16
Figure 5-9. Plotted ratio of Urban-to-Open field dose at 500 m radius from the detonation point, with points over building footprints in green.....	18
Figure 5-10. Plotted ratio of Urban-to-Open field dose at 1200 m radius from the detonation point, with points over building footprints in green .....	18
Figure 5-11. Variation of Urban-to-Open Field Total Absorbed Dose Ratio at 500 m from detonation location.....	19
Figure 5-12. Variation of Urban-to-Open Field Total Absorbed Dose Ratio at 1200 m from detonation location.....	19
Figure 5-13. Photon-to-neutron dose for urban and open field. ....	20
Figure 5-14. Total dose fall off for different quadrants compared to open field calculation .....	21

Figure 5-15. Dose map of Washington, D.C. showing areas of likely lethal levels of prompt radiation (red,  $> 8$  Gy), likely injury from prompt radiation alone (yellow,  $> 1$  Gy) and low probability of injurious health effects from radiation alone (green,  $< 1$  Gy)..... 22



## LIST OF TABLES

Table 4-1. Details of source spectra (White, 2001) .....	9
Table 5-1. Values for outside-of-buildings total dose ratio, converted to percentages .....	17
Table 5-2. Distance from detonation point to the LD50/60 and asymptomatic dose levels for the four urban quadrants and the open field calculations .....	21
Table A-1. Elemental weight fractions of air.....	32
Table B-1. Cross-section information for each element in simulation .....	33
Table C-1. List of different Hazus building types listed in model.....	34

THIS PAGE IS INTENTIONALLY LEFT BLANK.

## 1.0 INTRODUCTION

The threat of a detonation of a low-yield nuclear weapon in an urban setting has been described as the one of the most critical threats facing the U.S. As a result, the Department of Defense (DoD), Department of Energy (DoE) and Department of Homeland Security (DHS) are funding efforts to better understand the overall impacts of such an event. Within the DoD, the Defense Threat Reduction Agency (DTRA) safeguards America and its allies from Weapons of Mass Destruction; chemical, biological, radiological, and nuclear; and high explosives by providing capabilities to reduce, eliminate or counter the threat and mitigate its effects. One of DTRA's research and development efforts is to understand human survivability following a nuclear weapon detonation. The Human Survivability Research and Development (HSRD) integrated program team (IPT); composed of military, civilian, and contract scientists; has been chartered to lead this effort.

Despite the multitude of above ground nuclear tests conducted, insufficient information has been gathered on the effects of urban terrain on the air blasts, thermal fluences and ionizing radiation produced by a nuclear detonation. This report describes an HSRD model of the influence of buildings and urban terrain on the attenuation and transport of prompt ionizing radiation emitted from a nuclear detonation. This report does not specifically address latent radiation associated with fallout.

The neutron and photon prompt radiation presented in this report is but one of several potentially lethal prompt effects from a nuclear weapon. Injuries could also result from air blasts, building collapses, debris fragmentation, and thermal burns that could occur at varying distances from the detonation. The combined effect; of the prompt radiation, which has the capacity to injure at long distances, and these other types of injuries; has the potential to increase the overall lethality of a nuclear weapon detonation. Radiation injuries were responsible for the deaths of an estimated 5-15% of the people who survived the blast and thermal effects of the Hiroshima and Nagasaki attacks (Glasstone, 1977). Should a similar event occur in an urban setting, as described in this report, a better understanding of these radiation dose patterns and prompt modern medical care could translate into saving the lives of thousands of people.

THIS PAGE IS INTENTIONALLY LEFT BLANK.

## 2.0 MODEL DESCRIPTION

To calculate dose distributions in a particular environment, HSRD model translates an urban geometry to an input file (called an ‘input deck’) for the MCNP, Monte Carlo N-Particle, radiation transport code. MCNP is a general-purpose code designed to simulate neutron, photon, electron, or coupled neutron/photon/electron transport (X-5 Monte Carlo Team, 2008).

The urban geometry data is derived from LIDAR, which stands for light detection and ranging. The data contains the geo-referenced footprints, orientation, elevation, representative shape of each building’s shape at approximately 1 meter resolution. LIDAR is a commercially available, remote sensing technology that measures distance by illuminating a target with a laser and analyzing the reflected light. The data files are provided by the National Geospatial Intelligence Agency (NGA) in an ArcGIS data format (.shp). HSRD uses a Shapefile to MCNP Input Conversion Algorithm (Shape2MCNP); an ARA, Inc. copyrighted module created for use in Esri’s ArcMap<sup>TM1</sup>; to convert an entire map layer or a portion of a map layer into a three-dimensional matrix of voxels in MCNP’s input format.

In the calculations presented in the report, the building structures for the simulations are defined by a 3-D lattice with 5 m x 5 m x 5 m voxels. Our model of Washington, D.C. includes an additional improvement introduced by populating lattice elements of each building with different features depending on the particular building type from the Federal Emergency Management Agency (FEMA) Hazus (Hazards-US) dataset (Federal Emergency Management Agency 2003). There are sixteen different building types in the model, though only six were used in the section of Washington, D.C. modeled. The complete list of building types in the input deck is listed in Appendix C. A representation of the lattice used in the model is shown in Figure 2-1, excluding the ground and air; each color representing a different Hazus building type.

In the MCNP model, each building is assigned a specific Hazus building type. The assignment of Hazus values is a multistep process which begins by determining the city block (or equivalent) where the building is located. Figure 2-2 is an example set of buildings within their city blocks labeled with their reference number. The Hazus database lists the percentage of occupancy class for each city block, and the class with the highest percentage of residency is chosen as the occupancy class for that block (if there are equal percentages, the first one in the list is chosen). To determine the building type, additional information about the region and year of origin are extracted from tables in the Hazus-MH Earthquake Technical Manual (Federal Emergency Management Agency 2003) and combined with the occupancy class. The description of our models of the Hazus building types are listed in Appendix C.

---

<sup>1</sup> Esri is a commercial supplier of Geographic Information System software and geodatabase management applications.



**Figure 2-1. Washington, D.C. represented on a 3-D lattice model. The different colors correspond to different Hazus building types.**



**Figure 2-2. Example set of buildings and their city block labels from the FEMA Hazus database.**

Once the building type is determined, each voxel on the exterior portion of a building must be assigned from a list of 42 combinations of air and building elements. These voxels are chosen to approximate the composition, geometry and direction of the Hazus building type. Depending on the direction the wall faces, a script is used to examine the eight voxels that are horizontally and diagonally adjacent to each building element to decide which wall type needs to be included in that lattice element, shown in Figure 2-3. For example, the 3 m x 3 m square labeled '1', in the figure, is all building interior lattice elements and the 3 m x 3 m section labeled '4' represents the NW corner of a building with air lattice elements in the top three squares and the left three squares and building elements in the right hand bottom 2 m x 2 m square.

Figure 2-4 shows an example building as represented in MCNP. This shows the external walls with windows and gypsum drywall interior for a light-frame wood building. The ceilings are not shown. The exterior walls represent wood, 1.27 cm thick, with glass windows, 0.5 cm thick. A slab, 29.4 cm thick, with a bulk density to approximate air and wood represents the ceilings and floors. A room with no exterior walls has four doorways, 1 m wide by 4.7 m high, each leading into a different neighboring room. The rooms on the exterior of buildings have one to three inner doors, depending on number of exterior surfaces. The interior walls in this building type are composed of 2.54 cm thick gypsum. Each building type has similar levels of detail and approximations. Some also include interior support structures, such as steel framing, inside the rooms.

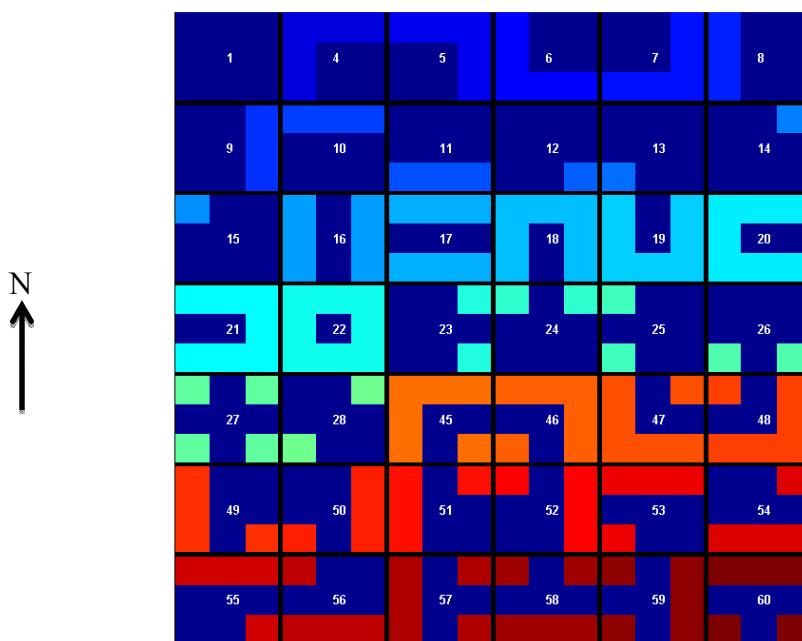


**Figure 2-3. Different combinations of building and air lattice elements which each contain different exterior wall arrangements.**

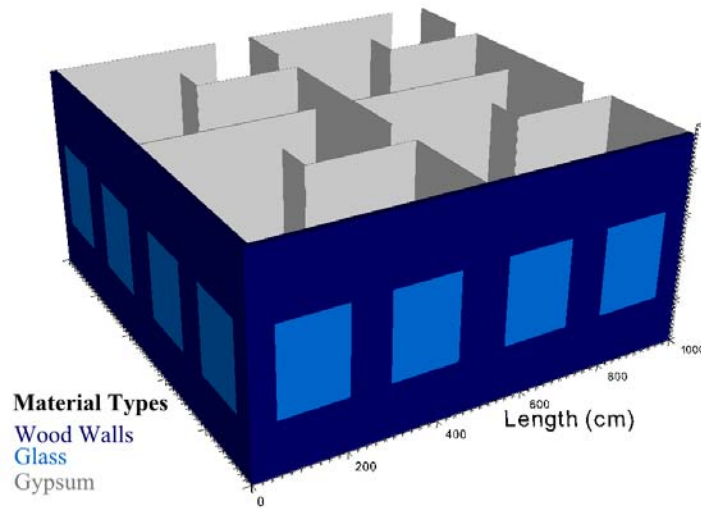


**Figure 2-4. An example section of a building model representing four different 5 m x 5 m x 5 m lattice elements.**

In addition to the building lattice, additional atmosphere layers composed of differing air density and humidity are placed to most accurately account for sky-shine (National Aeronautics and Space Administration 1976). These layers are specific to the city's location, and their composition is described in Appendix A. The ground underlying the buildings and the spaces in between them is specified to a depth of 10 m and is composed of concrete. Other terrain features such as mountains or hills are excluded from this model. In addition, the Potomac River and other bodies of water are not simulated in the model, since their effect is negligible due to their distance from the detonation.



### 3.0 NUMERICAL METHODS

The simulation results presented in this report were calculated with the radiation transport code MCNP5, v1.60. The simulations were run on the Department of Defense High-Performance Computing (HPC) systems (HPC Modernization Program 2013) which are large assemblies of parallelized computer processors. For each calculation, two runs were performed; one with a neutron source and one with a photon source (the details of the sources are presented in the next section). Both sources were run to ten billion event histories using the weight windows variance reduction technique.

On an HPC system, MCNP5 can take advantage of the message passing interface to run in parallel. Typically, a single simulation of this type, ten billion histories for both neutron and photon source simulations plus set-up runs, requires 6000 CPU-hours total. These statistics assure that the absorbed dose statistical error is less than 5% in areas where the total dose is greater than 0.05 Gy and less than 20% in all other areas surrounding the buildings.

MCNP5 provides a suite of variance reduction techniques to improve the efficiency of calculations. The simulations described in this report involve transporting particles over a large 3-D space, but the tally region, where the final results are extracted, comprises only a small fraction of that volume. To reduce computation time, the simulations were run with a variance reduction technique, weigh windows, that reduced the amount of time spent transporting particles that would not significantly contribute to the final calculations.

Weight windows divide the geometry into many regions and assigns each region a set of bounds that describes the region's importance to the problem. When a particle is transported into a region, its weight (loosely representing the particle flux or fluence in that area), is tested against the weight windows bound. If the particle's weight is higher than the window's upper bound, then the particle is split into several particles with lower weights that are within the bounds, conserving the total weight of the parent particle. If the particle's weight is below the window, a random number is tested to either kill the particle or increase its weight back into the weight window values (i.e. 'Russian roulette'). If the particle is between the two weight values of the window then it is transported normally. At the end of the source particle's history, which includes all the daughter particles transport, the contribution to the tally will automatically include the effects of this splitting and Russian roulette. With proper settings of the weights in a cylindrical weight windows scheme more particles are transported to regions distant to the detonation location, and thereby the statistical errors in the calculated doses are greatly decreased. This is at the expense of statistical error in the region close to the detonation point, but these are typically small, since all source particles start at a single point. Refer to the MCNP manual for a more complete description of weight window variance reduction methodology (X-5 Monte Carlo Team, 2008)

The bounding values of the weight windows were generated using the MCNP5 weight window generator. The simulation for generating weight windows is created with a 1 m tall tally cell centered 1 m above the ground surrounding the region. This tally records the energy deposited either by photons (if a photon source is used) or photons and neutrons (if a neutron source is used). Since both neutron and photon mesh tallies are used with the neutron source, the weight windows for both particle types were optimized simultaneously. With weight windows, the geometry of the problem is split into concentric cylinders with the axis centered at the

detonation location and pointed vertically. The spacing between cylinders is 40 m, which was chosen to be smaller than the mean free path of the typical neutron or photon in the simulation. Each space between cylinders is assigned a set of weight window bounds.

To generate weight windows, the simulation is first run without any assigned weight window bounds. This provides an initial guess of the weight window bounds. The weight window generator in MCNP5 only outputs the lower bound with the upper weight window bound being a set multiple of the lower bound (the default of 2 was used). These values are re-entered into the simulation and new weight windows are generated from the output results. This process is repeated until the new weight window bounds are within roughly 10% of the previous weight window values. Then mesh tallies are put into the simulation and the tally used to generate the weight window is removed – at which point the input deck is ready for a production run. The mesh tallies used are discussed in Section 5.1 RECTANGULAR MESH TALLY RESULTS. The weight window bounds used with the photon source in DC urban simulation is shown in Figure 3-1. In the figure, buildings are marked for reference and the dark circles indicate the boundaries of each weight window cylinder.

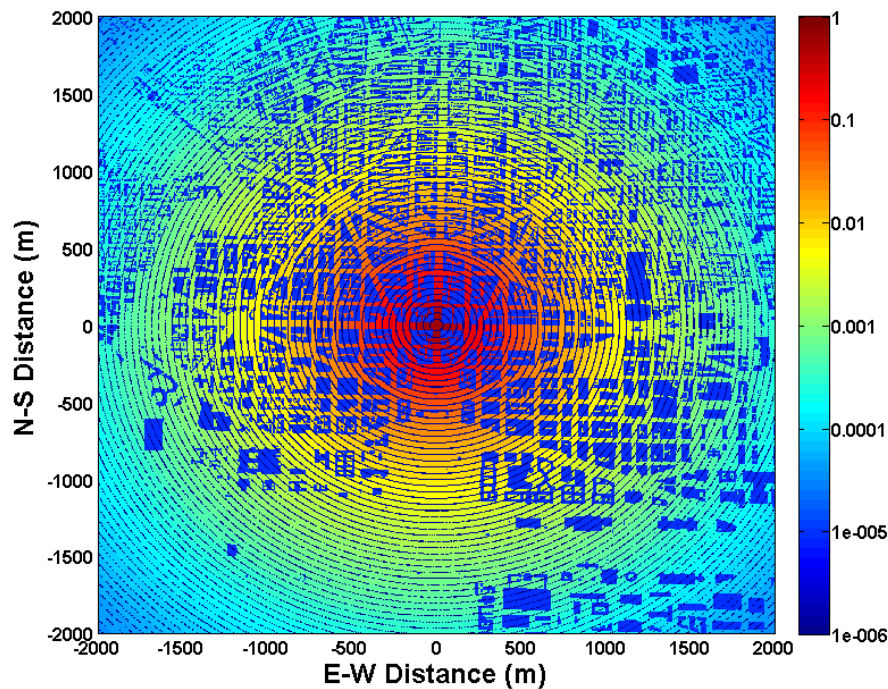


**Figure 3-1. Values of weight window lower bounds for DC urban simulation with the photon source.**

## 4.0 SOURCE DESCRIPTION

The unclassified source spectra of initial fission neutrons and gamma rays used in the HSRD MCNP model was an isotropic version of the Hiroshima device taken from spectra provided in the Radiation Effects Research Federation (RERF) Dosimetry System 2002 (DS02)(White 2001). These neutron and gamma spectra are shown in Figure 4-1 and Figure 4-2. The Hiroshima device was chosen because it represents a real, but unclassified device which represents a more realistic prompt radiation spectrum than would an idealized fission spectrum. However, the spectrum from the actual device was geometrically asymmetric, so the geometric dependence of the energy and intensity spectrum was averaged over. Also, the approximate yield of the Hiroshima device was renormalized to 10 kT from its nominal yield of 16.1 kT (White 2001) to match the first scenario in the DHS national planning scenarios (DHS, 2003). It should be noted that, due to the metal casing around the Hiroshima device, a considerable amount of the photon spectrum was filtered as compared to other fission devices.

The source was modeled in MCNP as a dimensionless point located 1 m above ground level at 38.902604 N latitude, 77.036574 W longitude.

**Table 4-1. Details of source spectra (White, 2001).**

Hiroshima (“Little Boy”)	Units	Value
Total neutrons	Moles/kT	0.1768
Average neutron energy	MeV	0.3106
Total gammas	Moles/kT	$6.665 \times 10^{-3}$
Average gamma energy	MeV	1.3979

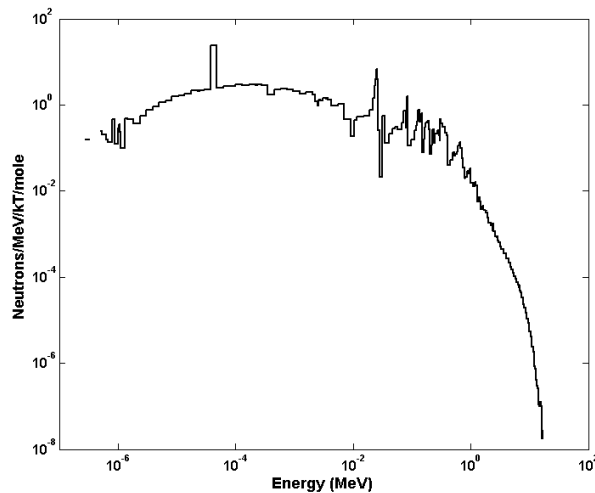


**Figure 4-1. Neutron energy spectrum used in simulation. Derived from isotropic version of Little Boy bomb used on Hiroshima (White, 2001).**

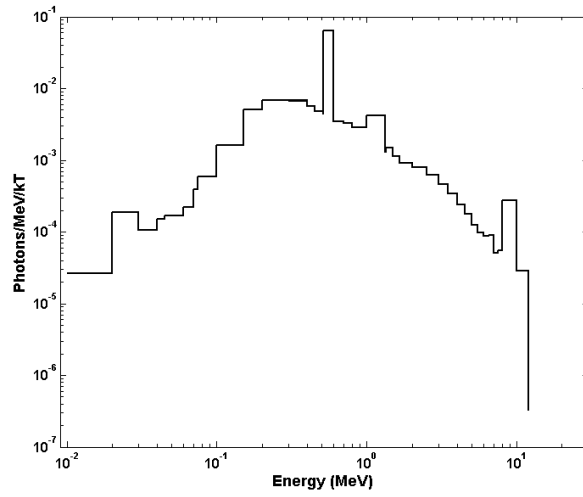


**Figure 4-2. Photon energy spectrum used in simulation. Derived from isotropic version of Little Boy bomb used on Hiroshima (White, 2001).**

## 5.0 RESULTS

Data derived from an MCNP calculation can be specified by a number of tallies that are available in the code. Rectangular mesh tallies were used in the HSRD model to calculate absorbed dose (Gy) from neutrons and photons. The rectangular mesh consists of a 2202-by-2202 array of 2 m x 2 m x 1 m voxels that are centered horizontally 1.0 m above ground level (center of voxel to ground level surface). The meshes were aligned in a north to south orientation.

Results from MCNP were initially in the form of particle fluence (particles/cm<sup>2</sup>), but were modified during the calculation with separate energy-dependent dose functions for neutrons and photons. Dose functions from ICRP-21 (ICRP, 1973) with energy-dependent neutron quality factors (Q) divided out were used in this model (quality factor for photons of all energies was 1). Tally values are therefore converted to absorbed dose in soft tissue per unit fluence: Gy/(particle/cm<sup>2</sup>).

Mesh tallies are independent of the model geometry in MCNP; i.e. a single mesh voxel may be intersected by different cells and/or materials. Therefore, doses are volume averaged within each mesh voxel. The energy-dependent dose conversion factors assume dose delivered to tissue. Values of dose evaluated in regions of building material are not doses to that specific material, but rather dose-to-tissue.

### 5.1 RECTANGULAR MESH TALLY RESULTS

The two rectangular mesh tallies provide visual representations of the propagation of neutron and photon radiation around and through the urban terrain. The sum of the two tallies is shown in Figure 5-1 for an in-the-open calculation and in Figure 5-2 for the previously described urban model. The individual neutron dose and photon dose, from both leakage photons and secondary photons from neutron interactions, are shown in Figure 5-3 and Figure 5-4. Also, doses lower than the lowest value of the scale (0.01 Gy) and higher than the highest value (10 Gy) exist, including values of zero where MCNP did not actually tally particles in mesh voxels. It should be noted that the simulation contains only buildings, air and ground surfaces.

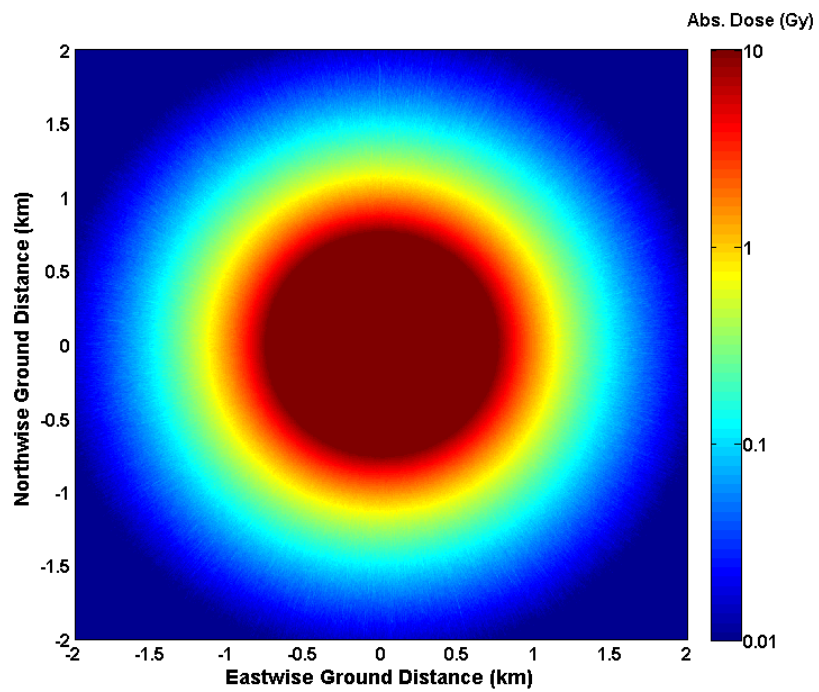


**Figure 5-1. Open field total absorbed dose**

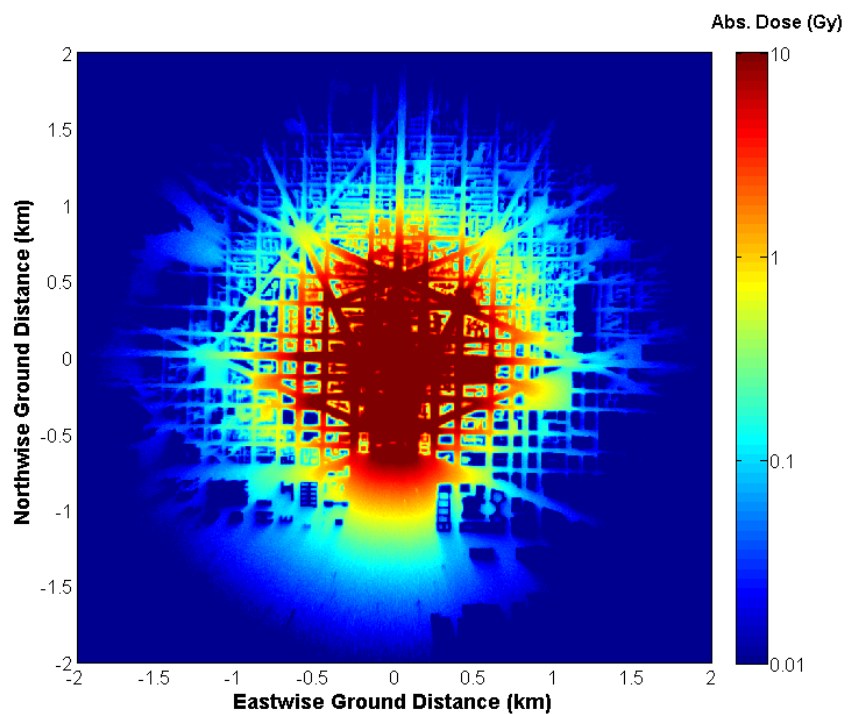


**Figure 5-2. Urban horizontal total absorbed dose**

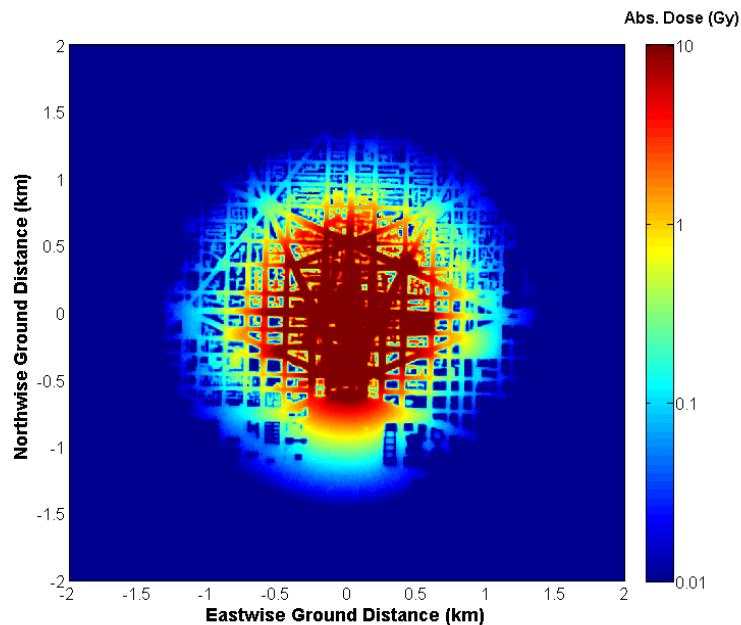


**Figure 5-3. Urban horizontal neutron absorbed dose**

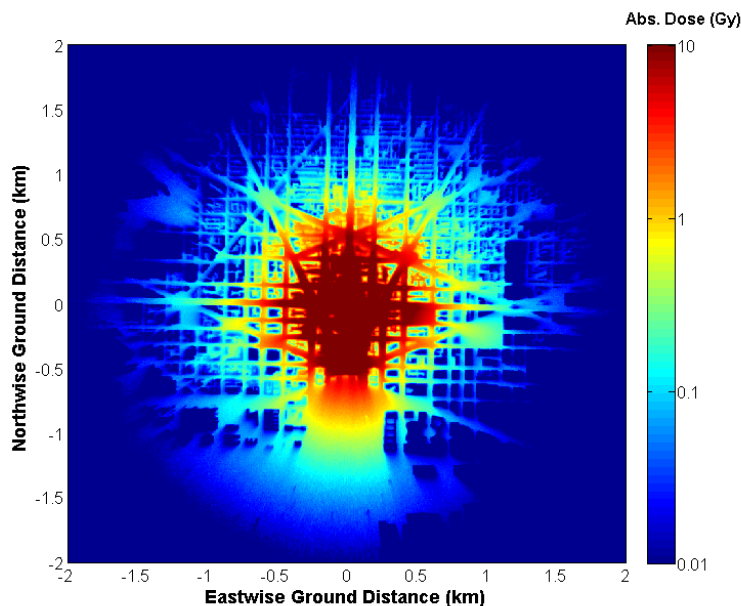


**Figure 5-4. Urban horizontal photon absorbed dose from both leakage photons and secondary photons from neutron interactions.**

Figure 5-5 shows the Urban-to-Open ratio of the total horizontal absorbed dose. The areas where there is a building have been cut out for clarity. The plot shows that areas that have higher building elevation, the Southeast section of the map for instance, are clearly attenuating the radiation more than in areas in the Northeast section. Near the center and in line-of-sight

from the detonation, there are increased dose levels due to albedo effects from the surrounding buildings.

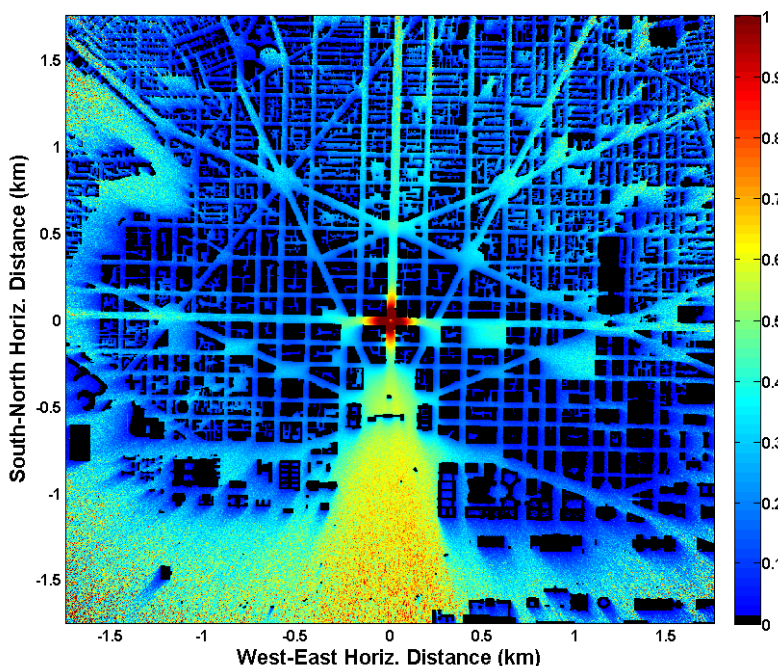


**Figure 5-5. The ratio of urban horizontal absorbed dose to open field horizontal absorbed dose.**

## 5.2 DATA ANALYSIS

To understand the heterogeneous nature of prompt radiation in an urban environment, it is useful to look at dose distributions at constant distances from the detonation point. In this analysis, we are more interested in the dose outside of buildings than the interior. The model provides an accurate representation of building shapes and sizes, and has a reasonable estimate of the building interiors. The variance reduction methods used in this analysis optimized the calculations necessary to estimate the dose to individuals outside of the buildings, so, the dose estimates inside of buildings are not of sufficient fidelity. However, future work could include using these same models, but with different variance reduction methods to estimate doses inside select buildings.

Tally results were determined using the 2 m x 2 m rectangular mesh tally at 1 m, and a MATLAB<sup>®</sup> script was used to calculate the doses at specific geometric locations. Figure 5-6 shows an elevation map of the National Capital Region, including a set of yellow lines used to illustrate the different quadrants in the analysis. The area is also broken up into four quadrants to demonstrate the effect of the heterogeneous urban environment. Areas in the footprint of buildings are excluded from the sample.



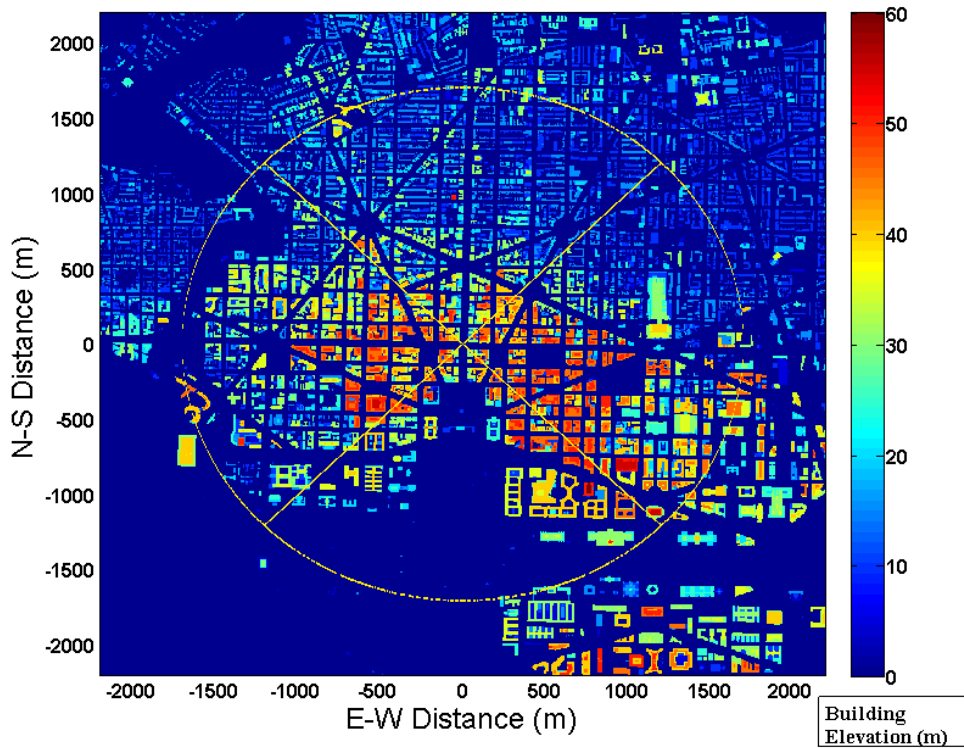


**Figure 5-6. The model's city geometry showing the buildings used to calculate the outside-of-building dose.**

Figure 5-7 shows the dose fall-off in the open-field and in the urban environment. The doses in the urban scenario exclude doses inside buildings.

Figure 5-8 shows the average over all four quadrants of the total Urban-to-Open field dose ratio outside building structures as a function of distance. The values of Figure 5-8 are also given in Table 5-1, showing the percent to which the dose is reduced in the urban landscape as compared to the open field. Because of the large number of low energy neutrons and photons, the values at 100 m were excluded because they were much higher (50-60%) and would have therefore skewed the average.

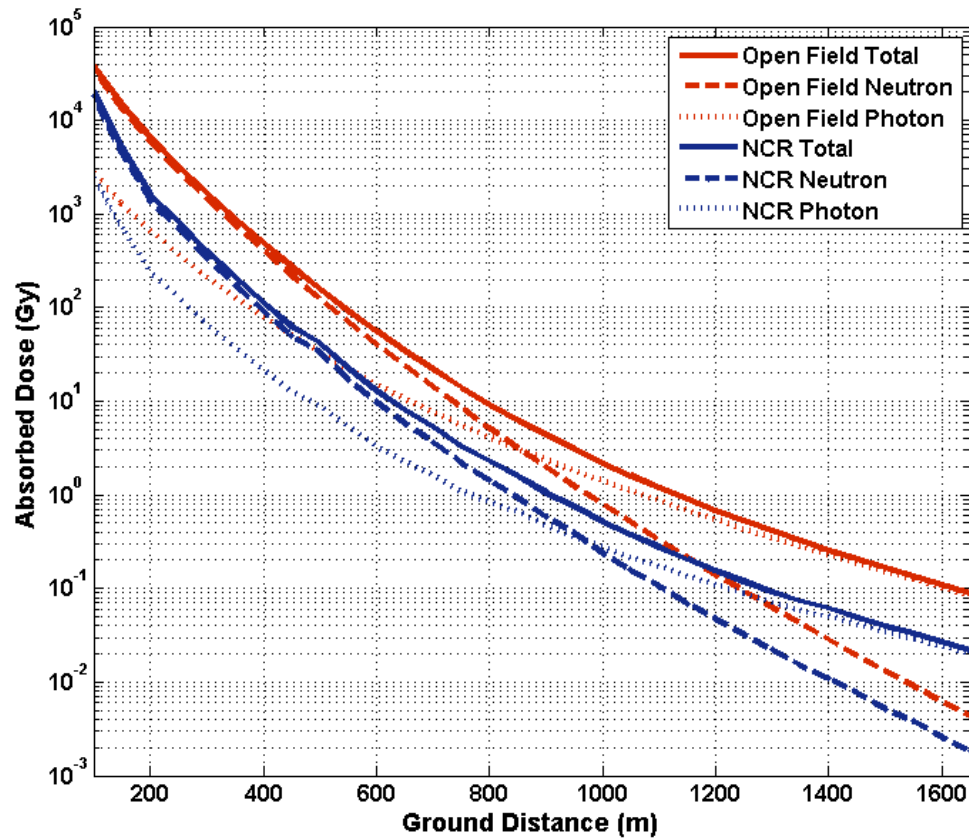


Figure 5-7. Open and outside-of-buildings urban scenario dose fall-offs.

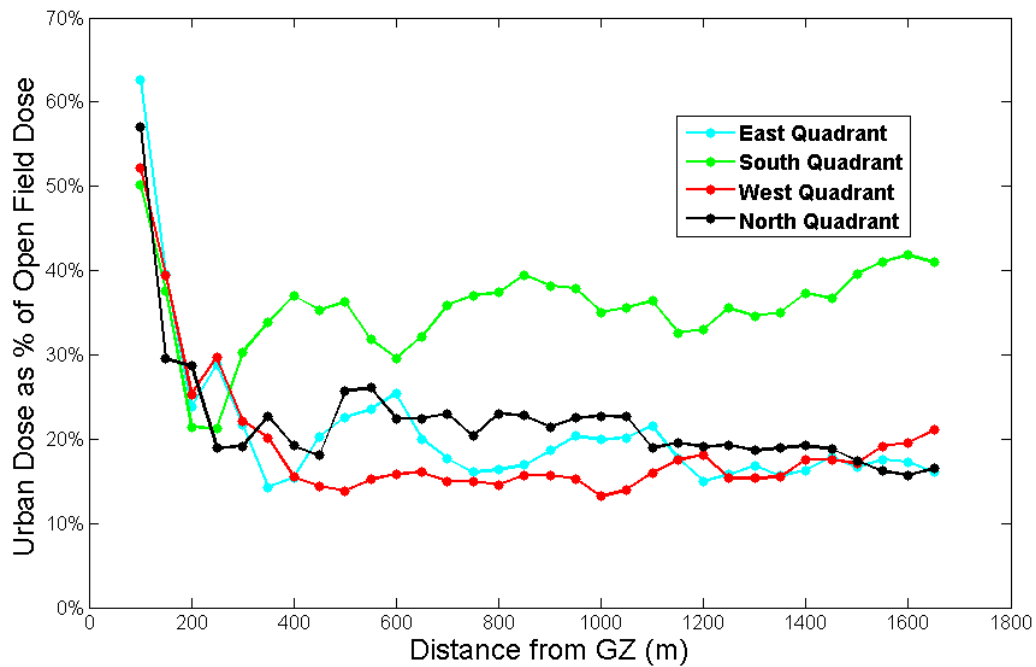
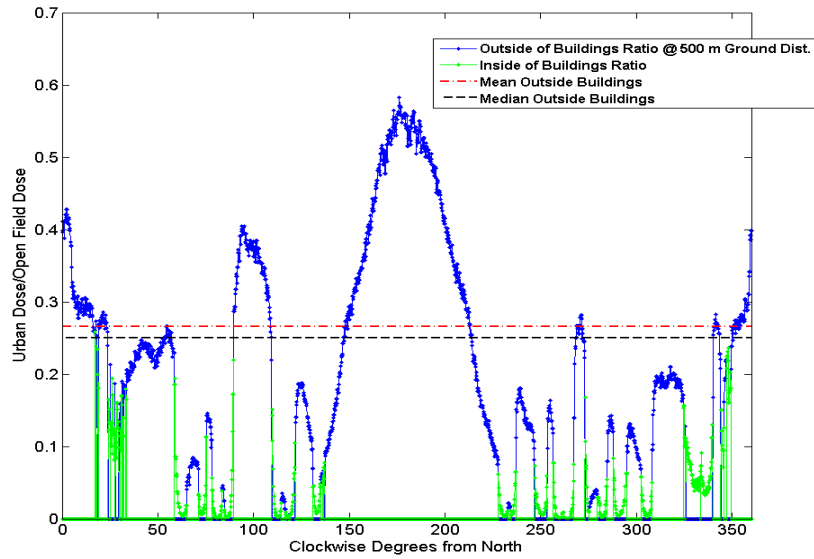


Figure 5-8. Total Urban-to-Open field dose ratio at locations outside buildings for the four quadrants from Figure 5-6.

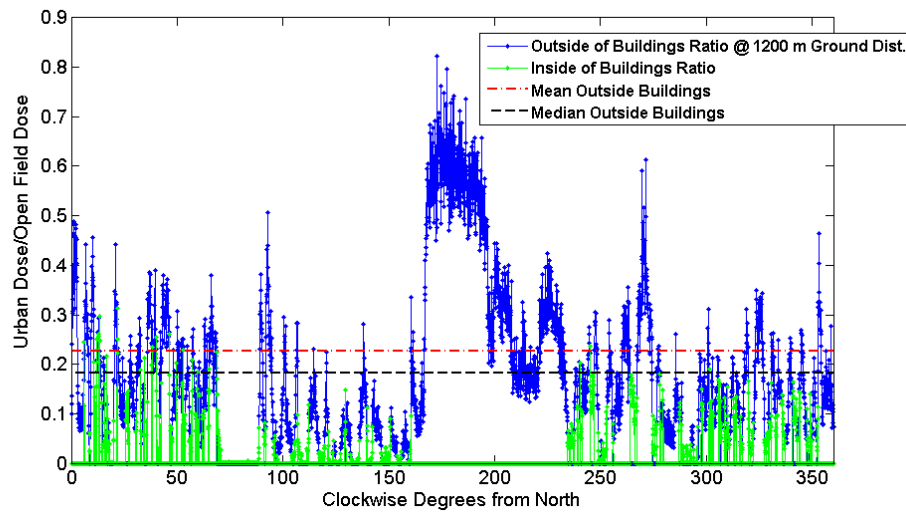
**Table 5-1. Values for outside-of-buildings total dose ratio, converted to percentages.**

	East Quadrant	South Quadrant	West Quadrant	North Quadrant
Distance (m)	Urban-to-Open ratio	Urban-to-Open ratio	Urban-to-Open ratio	Urban-to-Open ratio
200	23.8%	21.4%	25.3%	28.6%
300	21.7%	30.3%	22.1%	19.2%
400	15.4%	37.0%	15.5%	19.2%
500	22.6%	36.3%	13.9%	25.7%
600	25.4%	29.6%	15.8%	22.4%
700	17.7%	35.9%	15.0%	23.0%
800	16.4%	37.4%	14.6%	23.0%
900	18.6%	38.2%	15.7%	21.4%
1000	19.9%	35.0%	13.2%	22.8%
1100	21.6%	36.4%	16.0%	19.0%
1200	15.0%	33.0%	18.1%	19.1%
1300	16.9%	34.6%	15.3%	18.6%
1400	16.3%	37.3%	17.6%	19.2%
1500	16.7%	39.6%	17.1%	17.4%
1600	17.3%	41.8%	19.6 %	15.7%
Average	18.9%	35.0%	17.2%	20.6%

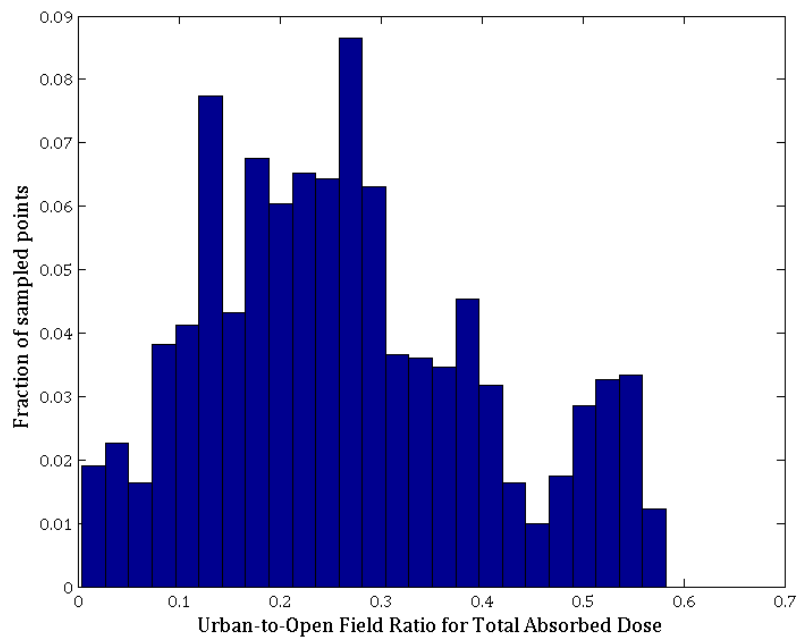
The heterogeneous nature of the data is amply demonstrated in Figure 5-9 and Figure 5-10. These plots show the Urban/Open ratio at individual points at radii of 500 meters and 1200 meters from the detonation. The x-axes correspond to the angles (degrees) at which the segments of the mesh tallies are situated. The 0<sup>th</sup> degree is aligned with the north compass direction and angles advance clockwise. Figure 5-11 and Figure 5-12 show the variation of the Urban-to-Open field total absorbed dose ratio at 500 m and 1200 m, respectively. The initial peak in the variation corresponds to the North, East and West quadrants and the second higher peak represents the emptier parts of the South quadrant.



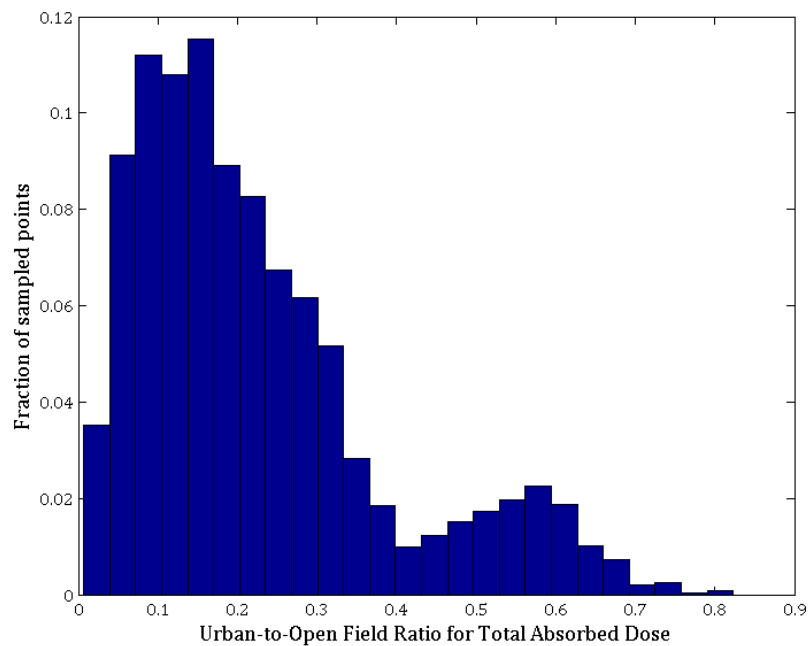
**Figure 5-9. Plotted ratio of Urban-to-Open field dose at 500 m radius from the detonation point, with points over building footprints in green.**



**Figure 5-10. Plotted ratio of Urban-to-Open field dose at 1200 m radius from the detonation point, with points over building footprints in green.**

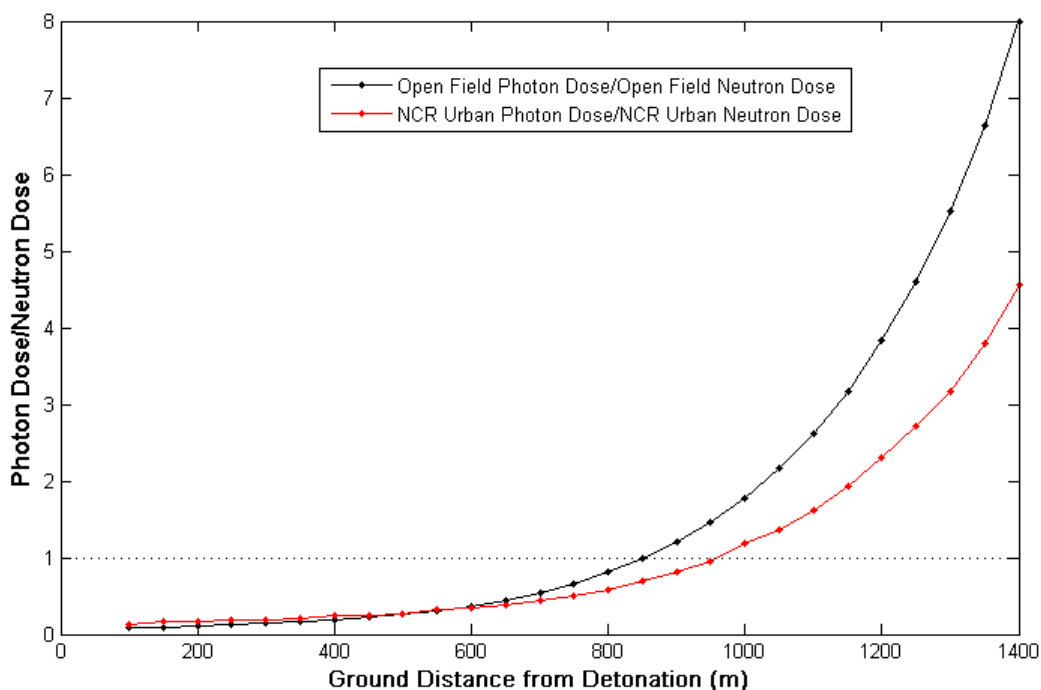


**Figure 5-11. Variation of Urban-to-Open Field Total Absorbed Dose Ratio at 500 m from detonation location**



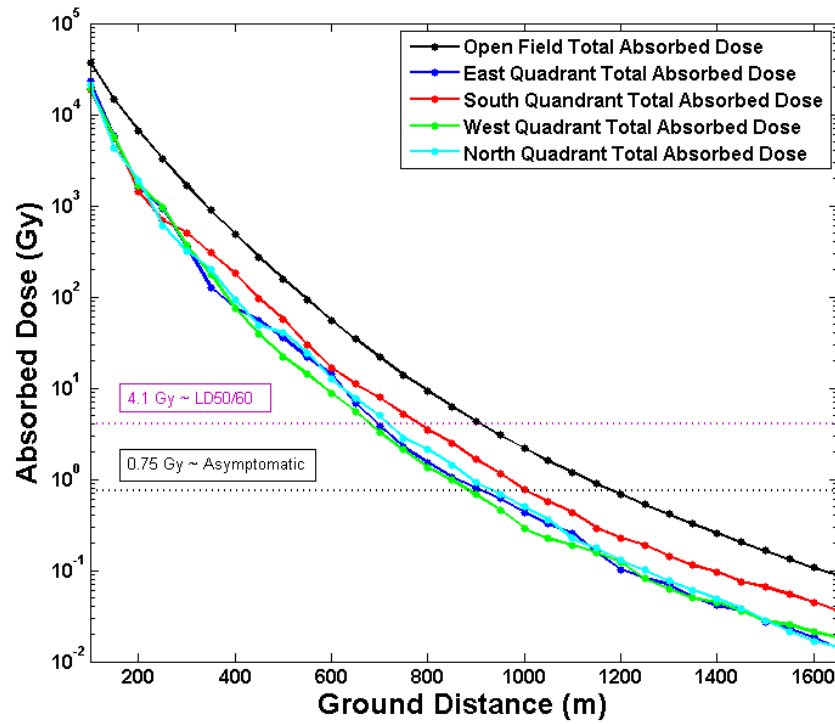
**Figure 5-12. Variation of Urban-to-Open Field Total Absorbed Dose Ratio at 1200 m from detonation location**

Figure 5-13 shows the photon-to-neutron ratio of doses in urban and open-field. The graph shows the radii at which the photon dose becomes larger than the neutron dose. As shown in the graph, the crossover point where the photon dose is equal to the neutron dose is approximately 850 meters in the open field; however, in the urban setting the crossover occurs closer to 950 meters.



**Figure 5-13. Photon-to-neutron dose for urban and open field.**

Figure 5-14 is a graph of the total dose fall-off as a function of the distance from the detonation point. The graph shows the dose in each of the individual four directional quadrants mentioned in Figure 5-6. Table 5-2 shows a list of interpolated distances from the detonation point at which the dose is at a point of biological interest. The LD50/60 level (4.10 Gy) is considered to be where 50% of the exposed population will die within 60 days of exposure. The asymptomatic level (0.75 Gy) is considered the lower dose threshold of the presence of symptoms from acute radiation syndrome. The pathways with more direct line of sight or with significant open space, for instance in the South quadrant, will have less dramatic dose fall-offs than those that mostly consist of urban building structures.



**Figure 5-14. Total dose fall off for different quadrants compared to open field calculation.**

**Table 5-2. Distance from detonation point to the LD50/60 and asymptomatic dose levels for the four urban quadrants and the open field calculations.**

		Quadrants of NYC			
Dose (Gy)	Open Field (m)	East (m)	South (m)	West (m)	North (m)
4.10 (~LD50/60)	908	696	781	631	720
0.75 (~Asymptomatic)	1183	915	1004	888	935

The differences in the biological effects of neutron radiation as compared to photon radiation are known but difficult to quantify, as the literature on neutron deterministic effects is sparse. Nevertheless, one can make a crude estimate of the total equivalent dose based on the information available. Figure 5-15 is an estimate of different prompt radiation injury zones using the absorbed dose calculations made in this report and applying the formula:

$$D_{EQ} = C_{int} (Q_n d_n + Q_\gamma d_\gamma)$$

where  $D_{EQ}$  is the equivalent total prompt radiation dose,  $C_{int}$  is an estimated conversion factor from an external tissue dose to a midline internal tissue dose (the value used was 0.7) (Goetz, 1979),  $Q_n$  is the quality factor for the neutron (the value used was 3.0 Sv/Gy from studies of

neutron deterministic effects to the gastrointestinal tract) (ICRP, 1989),  $d_n$  is the neutron absorbed dose calculated in this report,  $Q_\gamma$  is the quality factor for the photon (where the value of 1 Sv/Gy is used) and  $d_\gamma$  is the total photon absorbed dose calculated in this report. The three color regions shown in Figure 5-15 refer to high probability of lethal dose from prompt radiation (shown in red, defined as  $> 8$  Gy equivalent dose), high probability of acute injury due to prompt radiation (shown in yellow,  $> 1$  Gy equivalent dose) and low probability of acute injury from prompt radiation alone (shown in green,  $< 1$  Gy equivalent dose).

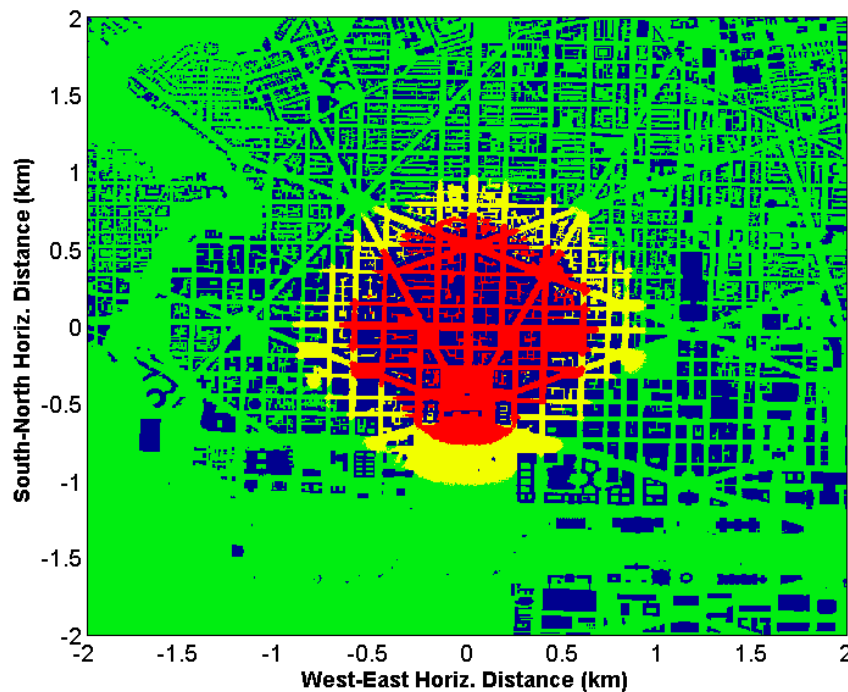


**Figure 5-15. Dose map of Washington, D.C. showing areas of likely lethal levels of prompt radiation (red,  $> 8$  Gy), likely injury from prompt radiation alone (yellow,  $> 1$  Gy) and low probability of injurious health effects from radiation alone (green,  $< 1$  Gy).**



## **6.0 DISCUSSION**

### **6.1 ANALYSIS OF DOSE REDUCTION**

The results presented in this report indicate that the radiation transport in the National Capital Region urban setting is more attenuated than previous estimates (Dombroski, 2007). The previous estimates determined that the urban environment reduced the radiation to 30% of the open field radiation. However, the HSRD model revealed that dose reduction is clearly a function of the intervening buildings, as areas of elevated building heights show higher radiation attenuation than areas of lower average building elevation. The model also shows relatively open areas, such as the area in the southern part of the HSRD model, still being significantly attenuated by lack of scattering from more built-up areas. There are simulated areas where the urban dose is higher than the open field dose, but only in areas very near the detonation where scattering from buildings is significant.

The impact of the urban landscape can reduce the range of a lethal radiation exposure from the initial radiation from approximately 1183 meters to 888 meters in the West Quadrant and from approximately 1183 meters to 1004 meters in the South Quadrant. In a high-density population center such as Washington, DC, this change can reduce the radiation and combined injury casualties by thousands of people. The dose reduction estimates should not be used without an acknowledgement of the variability in the data at any given distance as clearly shown in Figure 5-9 and Figure 5-10. While the mean results can be useful for general planning purposes, emergency response planners should expect that individuals in the more direct line of sight and low-scattering locations could receive significantly higher doses than the average would indicate.

### **6.2 RECOGNIZED HSRD MODEL LIMITATIONS**

While the scale and detail of this model representing an urban terrain may be the most complete representation ever developed for use with MCNP, it still has several limitations which should be recognized when evaluating the results presented in this report. The building materials are still a simple approximation and are not customized for any particular building, even though the buildings do adhere to simple generic Hazus building types. Also, interior details are not accurately specified, especially when considering the turnover of materials as buildings are renovated. Subterranean systems such as culverts, sewers, mass transit and maintenance tunnels are also not included. The building resolution of 5 m x 5 m x 5 m can overestimate the size of the buildings since partially filled lattice elements could be completely filled with building materials.

### **6.3 ABSORBED DOSE VERSUS EQUIVALENT DOSE**

MCNP can conveniently tally energy dependent equivalent dose (Sv); however for the model presented here, an absorbed dose (Gy) was deemed the most appropriate value to calculate. The use of absorbed dose allowed for direct comparison of neutron and photon doses, and allowed the doses to be summed to calculate total dose. Further, the primary concern of this work was to best understand the impacts of an urban nuclear weapon detonation as associated with the possibility of acute radiation effects. Equivalent dose calculations for acute effects are a

very complicated set of calculations and the simplified conversion factors that are typically used are not appropriate.

Absorbed dose was calculated by dividing out the energy dependent quality factors from the dose conversion coefficients before running the model. It should be noted, though, that the resulting absorbed dose is absorbed dose in tissue, as the conversion factors were originally calculated based on tissue dose.

## 7.0 CONCLUSIONS

The results presented in this report suggest the following conclusions based upon the HSRD Monte Carlo modeling of the initial radiation emitted by the detonation of a 10 kT-yield fission-type nuclear weapon located at ground level in Washington, D.C.:

- *Dose Contribution* – For the modeled source spectra at near distances, neutrons are the main contributor to dose as demonstrated in Figure 5-13. However, as expected, at increasing distances in both the urban and open-field scenarios, neutron and photon doses begin to converge until the photon dose becomes the greater contributor to the total dose (in this model, the average dose for neutrons and photons is equal at the 950 m radius).
- *Photon to Neutron Dose* – In the Hiroshima event, very little evidence of injuries from deterministic effects of high-neutron doses has been discovered. However, these simulations show similar levels of dose from photons and neutrons in the survivable injury zone, even without incorporating relative biological effectiveness or quality factors. The effects of large neutron radiation doses may play an important role in consequence assessment calculations applicable to this sort of event.
- *Sky-Shine Dose* – “Sky-shine”, i.e. atmospheric back-scattering of radiation, appears to be dependent on building height. This conclusion can be made by the qualitative observation of Figure 5-5, which serves to depict the total urban-to-open field dose ratio plot. It is clearly seen that the ratio value is higher on the South quadrant of the plot, corresponding to open spaces, than the East quadrant, where taller buildings dominate. These taller structures effectively shield downward-scattered radiation from the atmosphere. For the regions of the model of the National Capital Region where there was significant building density, the dose was calculated to be reduced, on average, to approximately 17% to 21% of the open-field calculation.

THIS PAGE IS INTENTIONALLY LEFT BLANK.

## **8.0 ACKNOWLEDGEMENTS**

We would like to express utmost gratitude to Tim Goorley of Los Alamos National Laboratories. His assistance in running MCNP5 on high-performance computers, sharing input decks of similar problems and reviewing this final document proved to be invaluable.

THIS PAGE IS INTENTIONALLY LEFT BLANK.

## 9.0 REFERENCES

DHS. *National Preparedness Guidelines*. Washington, DC, 2003.

Dombroski, Matt, et al. *Radiological and Nuclear Response and Recover Workshop: Nuclear Weapon Effects in the Urban Environment*. Livermore, CA: Lawrence Livermore National Laboratories, 2007.

Federal Emergency Management Agency. *Multi-hazard loss estimation methodology, flood model, HAZUS, technical manual*. technical manual, Washington, DC: Department of Homeland Security, Emergency Preparedness and Response Directorate., 2003.

Glasstone, S. and Dolan, P. J. *The Effects of Nuclear Weapons*. United States Department of Defense and United State Department of Energy, 1977.

Goetz, J.L., Klemm, J., Kaul, D. and McGahan, J. T. *Analysis of Radiation Exposure for Task Force Warrior - Shot Smoky - Exercise Desert Rock VII-VIII Operation Plumbbob*. Washington, D.C.: Defense Nuclear Agency, 1979.

HPC Modernization Program. "HPCMPO Overview 2013 v2." *HPCMP community resources*. June 1, 2013. <http://www.hpcmo.hpc.mil/cms2/index.php/communityresources> (accessed July 1, 2013).

ICRP (International Commission on Radiological Protection). *Data for Protection Against Ionizing from External Sources - Supplement to ICRP 15 (ICRP 21)*. Oxford, UK: Pergamon Press, 1973.

ICRP (International Commission on Radiological Protection). *RBE for Deterministic Effects*. Vol. 58. Oxford: Pergamon Press, 1989.

Johnson, J. *Determination of Atmospheric Conditions over New York City*. Private Communication, 2010.

National Aeronautics and Space Administration. "U. S. Standard Atmosphere, 1976." Washington, DC, 1976.

White, S. W., Whalen, P. P., and Heath, A. R. *Source Calculations for the US-Japan Dosimetry Working Group; LA-UR-01-6594*. Los Alamos, NM: Los Alamos National Laboratory, 2001.

X-5 Monte Carlo Team,. *MCNP - A General Monte Carlo N-Particle Transport code, Version 5 (LA-UR-03-1987)*. Los Alamos, NM: Los Alamos National Laboratory, 2008.

THIS PAGE IS INTENTIONALLY LEFT BLANK.



## **APPENDICES**

## A. ATMOSPHERIC COMPOSITION AND DENSITY

The elemental weight fractions of air in and around structures was defined by NIST (National Institute of Standards and Technology), as was the density of  $1.20479 \times 10^{-3} \text{ g/cm}^3$  for dry air at sea level. These established measurements were adjusted for water vapor content and density based on elevation as per formulas from “Determination of Atmospheric Conditions over New York City”.

**Table A-1. Elemental weight fractions of air.**

Element	Air @0-250m ( $1.205 \times 10^{-3} \text{ g cm}^{-3}$ )	Air @ 250-500 m ( $1.205 \times 10^{-3} \text{ g cm}^{-3}$ )	Air @ 500-750 m ( $1.167 \times 10^{-3} \text{ g cm}^{-3}$ )	Air@ 750-1000 m ( $1.117 \times 10^{-3} \text{ g cm}^{-3}$ )	Air @ 1000-1500 m ( $1.092 \times 10^{-3} \text{ g cm}^{-3}$ )
H	0.001459	0.001490	0.001524	0.001560	0.001614
O	0.240904	0.24108	0.241215	0.241505	0.24183
C	0.000125	0.000124	0.000127	0.000124	0.000123
N	0.744888	0.744683	0.744224	0.744199	0.743823
Ar	0.012625	0.012624	0.012911	0.012613	0.01261

Element	Air@ 1500-2000 m ( $1.055 \times 10^{-3} \text{ g cm}^{-3}$ )	Air @ 2000-2500 m ( $0.958 \times 10^{-3} \text{ g cm}^{-3}$ )	Air @ 2500-3000 m ( $0.911 \times 10^{-3} \text{ g cm}^{-3}$ )	Air @ 3000 - 3500 m ( $0.866 \times 10^{-3} \text{ g cm}^{-3}$ )
H	0.001665	0.001439	0.001237	0.001058
O	0.242122	0.240772	0.239596	0.23852
C	0.000123	0.000125	0.000125	0.000124
N	0.743489	0.745035	0.74639	0.747624
Ar	0.01260	0.01263	0.012652	0.012673

## B. MCNP PHYSICS OPTIONS

Certain physics options available in MCNP were adjusted to optimize run time and to correctly model nuclear interactions. A 1.0 keV threshold was employed, which artificially removed all photons below this energy from the model. The minimum neutron energy cut-off was determined by the implicit capture model in MCNP. Analog capture was turned off for both photons and neutrons. The cross-section tables used for each element are listed in Table B-1.

**Table B-1. Cross-section information for each element in simulation**

Element Name – Atomic Number	MCNP Reference	Cross-section Filename
Hydrogen - 1	1001.70c	ENDF/B-VII njoy99.248
Carbon - Natural Isotope Mix	6000.70c	ENDF/B-VII njoy99.248
Carbon - 12	6012.50c	RMCCS njoy
Nitrogen – 14	7014.70c	ENDF/B-VII njoy99.248
Oxygen – 16	8016.70c	ENDF/B-VII njoy99.248
Sodium - 11	11023.70c	ENDF/B-VII njoy99.248
Aluminum - 13	13027.70c	ENDF/B-VII njoy99.248
Silicon - Natural Isotope Mix	14000.60c	ENDF/B-VI
Sulfur – Natural Isotope Mix	16000.62c	ENDF/B-VI.8 njoy99.50
Argon – Natural Isotope Mix	18000.35c	ENDL85
Potassium – Natural Isotope Mix	19000.62c	ENDF/B-VI.8 njoy99.50
Calcium – Natural Isotope Mix	20000.62c	ENDF/B-VI.8 njoy99.50
Iron – Natural Isotope Mix	26000.55c	RMCCS njoy

## C. HAZUS BUILDING TYPES

A list of the Hazus building types used by the HSRD Shape2MCNP and MCNP input decks is given in Table C-1. The table lists the Hazus label, an HSRD No. which is given for reference, a description and a concise list of important dimensions.

**Table C-1. List of different Hazus building types listed in model.**

Hazus Label	HSRD No.*	Description	Physical Dimensions
W1	4	Wood, Light Frame	Glass=0.5 cm
W2	5	Wood, Commercial and Industrial	Glass=0.5 cm
S1L,S1M,S1H	6	Steel Moment Frame	Concrete floors=8 in, Steel Columns=10 in, Glass = 1 cm
S2L,S2M,S2H	7	Steel Braced Frame	Concrete floors=8 in, Steel Columns=10 in, Glass = 1 cm
S3	8	Steel Light Frame	Concrete floors=8 in, Steel Columns=10 in, Corrugated metal walls=0.2 cm
S4L,S4M,S4H	9	Steel Frame with Cast-in-Place Concrete Shear Walls	Concrete floors=8 in, Steel Columns=10 in, Glass = 1 cm
S5L,S5M,S5H	10	Steel Frame with Unreinforced Masonry Infill Walls	Concrete floors=8 in, Steel Columns=10 in, Glass = 0.1 cm, brick walls=9 cm
C1L,C1M,C1H	11	Concrete Moment Frame	Concrete floors=8 in, Steel Columns=10 in, Glass = 1 cm
C2L,C2M,C2H	12	Concrete Shear Walls	Concrete floors=8 in, Steel Columns=10 in, Glass = 1 cm
C3L,C3M,C3H	13	Concrete Frame with Unreinforced Masonry Infill Walls	Concrete floors=8 in, Exterior Bricks Walls=9 cm, Glass = 0.5 cm

PC1	14	Precast Concrete Tilt-Up Walls	Wood Floors=5.75 in, Steel Columns=10 in, Glass=1 cm
PC2L,PC2M,PC2H	15	Precast Concrete Frames with Concrete Shear Walls	Concrete Floors=8 in, Glass=1 cm
RM1L, RM1M	16	Reinforced Masonry Bearing Walls with Wood or Metal Deck Diaphragms	Wood Floors=5.75 in, Steel Columns=10 in, Glass=1 cm
RM2L, RM1M, RM2H	17	Reinforced Masonry Bearing Walls with Precast Concrete Diaphragms	Concrete Floors=8 in, Glass=1 cm
URML,URMM	18	Unreinforced Masonry Bearing Walls	Wood=5.75 in, Wood Columns=12 in, Brick Exterior Walls=9 cm, Glass=0.5 cm
MH		Mobile Homes	Same as Wood, Light Frame, Glass=0.5 cm

## **D. ABBREVIATIONS, ACRONYMS AND SYMBOLS**

ARA	Applied Research Associates, Inc.
ArcGIS	A commercially available Geographic Information System from Esri
DHS	Department of Homeland Security (United States)
DOD	Department of Defense (United States)
DOE	Department of Energy (United States)
DTRA	Defense Threat Reduction Agency (United States)
FEMA	Federal Emergency Management Agency (United States)
Gy	gray
HSRD	Human Survivability Research and Development Integrated Program Team
ICRP	International Commission on Radiological Protection
IPT	Integrated Program Team
kg	kilogram
km	kilometer
LD50/60	Lethal Dose for 50% of population after 60 days
LIDAR	Light Radar, a remote sensing technology
m	meter
MCNP	Monte Carlo N-Particle radiation transport software
NGA	National Geospatial Agency
Sv	Sievert
U.S.	United States